AFRL-AFOSR-VA-TR-2019-0304

Fundamental Studies of Heavy Metal Oxide Glasses for High Power Lasers: Microstructural Aspects of Er Clustering and Absorption Profile Variations Related to Photodarkening

Kristina Lipinska
UNIVERSITY OF NEW MEXICO

10/04/2019
Final Report

Air Force Research Laboratory
AF Office Of Scientific Research (AFOSR)/ RTB1
Arlington, Virginia 22203
Air Force Materiel Command

REPORT DOCUMENTATION PAGE

Form Approved
OMB No. 0704-0188

PLEASE DO NOT RETURN YOUR FORM TO THE ABOVE ADDRESS.

1. REPORT DATE *(DD-MM-YYYY)*	2. REPORT TYPE	3. DATES COVERED *(From - To)*
27-09-2019	Final Performance Report	07/01/2016 - 06/30/2019

4. TITLE AND SUBTITLE

Fundamental Studies of Heavy Metal Oxide Glasses for High Power Lasers

5a. CONTRACT NUMBER

5b. GRANT NUMBER

FA9550-16-1-0242

5c. PROGRAM ELEMENT NUMBER

6. AUTHOR(S)

Dr. Kris Lipinska

5d. PROJECT NUMBER

5e. TASK NUMBER

5f. WORK UNIT NUMBER

7. PERFORMING ORGANIZATION NAME(S) AND ADDRESS(ES)

UNIVERSITY OF NEW MEXICO
OFFICE OF SPONSORED PROJECTS
1700 LOMAS BLVD NE
ALBUQUERQUE NM 87106-3807

8. PERFORMING ORGANIZATION REPORT NUMBER

n/a

9. SPONSORING/MONITORING AGENCY NAME(S) AND ADDRESS(ES)

USAF, AFRL DUNS 143574726
AF OFFICE OF SCIENTIFIC RESEARCH
875 NORTH RANDOLPH STREET, RM 3112
ARLINGTON VA 22203-1954
ERNA PETRICH 703-696-6563

10. SPONSOR/MONITOR'S ACRONYM(S)

n/a

11. SPONSOR/MONITOR'S REPORT NUMBER(S)

n/a

12. DISTRIBUTION/AVAILABILITY STATEMENT

Distribution A - Approved for Public Release

13. SUPPLEMENTARY NOTES

n/a

14. ABSTRACT

High-power, rare-earths (REs) doped fiber lasers with a glass-based functional core are used in numerous commercial applications, such as telecommunications, as well as in those relevant to DoD missions. When considering REs-doped glasses for high-power laser applications, the phenomenon of photodarkening remains the key issue in limiting a fiber's optical performance. Photodarkening is an irradiation-induced gradual increase of a glass fiber's absorption, which reduces its light transmission capability and decreases the fiber's power output over time. Several explanations have been given so far that are either inspired by experimental observations or aimed at rationalizing experimental findings.

In this project, and in relation to photodarkening, we address the missing links connecting: on one side glass chemistry and glass network microstructure, including local structural environment around selected atoms, and on the other side rare-earths clustering effects and optical transmission losses. This is achieved by leveraging a multi-technique experimental approach.

15. SUBJECT TERMS

glasses, microstructure, defects, laser-irradiation, rare-earths, concentration quenching, photodarkening, luminescence

16. SECURITY CLASSIFICATION OF:			17. LIMITATION OF ABSTRACT	18. NUMBER OF PAGES	19a. NAME OF RESPONSIBLE PERSON
a. REPORT	b. ABSTRACT	c. THIS PAGE			19b. TELEPHONE NUMBER *(Include area code)*
U	U	U	UU	15	

Reset

Standard Form 298 (Rev. 8/98)
Prescribed by ANSI Std. Z39.18

INSTRUCTIONS FOR COMPLETING SF 298

1. REPORT DATE. Full publication date, including day, month, if available. Must cite at least the year and be Year 2000 compliant, e.g. 30-06-1998; xx-06-1998; xx-xx-1998.

2. REPORT TYPE. State the type of report, such as final, technical, interim, memorandum, master's thesis, progress, quarterly, research, special, group study, etc.

3. DATES COVERED. Indicate the time during which the work was performed and the report was written, e.g., Jun 1997 - Jun 1998; 1-10 Jun 1996; May - Nov 1998; Nov 1998.

4. TITLE. Enter title and subtitle with volume number and part number, if applicable. On classified documents, enter the title classification in parentheses.

5a. CONTRACT NUMBER. Enter all contract numbers as they appear in the report, e.g. F33615-86-C-5169.

5b. GRANT NUMBER. Enter all grant numbers as they appear in the report, e.g. AFOSR-82-1234.

5c. PROGRAM ELEMENT NUMBER. Enter all program element numbers as they appear in the report, e.g. 61101A.

5d. PROJECT NUMBER. Enter all project numbers as they appear in the report, e.g. 1F665702D1257; ILIR.

5e. TASK NUMBER. Enter all task numbers as they appear in the report, e.g. 05; RF0330201; T4112.

5f. WORK UNIT NUMBER. Enter all work unit numbers as they appear in the report, e.g. 001; AFAPL30480105.

6. AUTHOR(S). Enter name(s) of person(s) responsible for writing the report, performing the research, or credited with the content of the report. The form of entry is the last name, first name, middle initial, and additional qualifiers separated by commas, e.g. Smith, Richard, J, Jr.

7. PERFORMING ORGANIZATION NAME(S) AND ADDRESS(ES). Self-explanatory.

8. PERFORMING ORGANIZATION REPORT NUMBER. Enter all unique alphanumeric report numbers assigned by the performing organization, e.g. BRL-1234; AFWL-TR-85-4017-Vol-21-PT-2.

9. SPONSORING/MONITORING AGENCY NAME(S) AND ADDRESS(ES). Enter the name and address of the organization(s) financially responsible for and monitoring the work.

10. SPONSOR/MONITOR'S ACRONYM(S). Enter, if available, e.g. BRL, ARDEC, NADC.

11. SPONSOR/MONITOR'S REPORT NUMBER(S). Enter report number as assigned by the sponsoring/ monitoring agency, if available, e.g. BRL-TR-829; -215.

12. DISTRIBUTION/AVAILABILITY STATEMENT. Use agency-mandated availability statements to indicate the public availability or distribution limitations of the report. If additional limitations/ restrictions or special markings are indicated, follow agency authorization procedures, e.g. RD/FRD, PROPIN, ITAR, etc. Include copyright information.

13. SUPPLEMENTARY NOTES. Enter information not included elsewhere such as: prepared in cooperation with; translation of; report supersedes; old edition number, etc.

14. ABSTRACT. A brief (approximately 200 words) factual summary of the most significant information.

15. SUBJECT TERMS. Key words or phrases identifying major concepts in the report.

16. SECURITY CLASSIFICATION. Enter security classification in accordance with security classification regulations, e.g. U, C, S, etc. If this form contains classified information, stamp classification level on the top and bottom of this page.

17. LIMITATION OF ABSTRACT. This block must be completed to assign a distribution limitation to the abstract. Enter UU (Unclassified Unlimited) or SAR (Same as Report). An entry in this block is necessary if the abstract is to be limited.

Final Performance Report

Award No: FA9550-16-1-0242
Funding: Dr. Ali Sayir, AFOSR/RTB, Air Force Office of Scientific Research (AFOSR),
Project Title: Fundamental Studies of Heavy Metal Oxide Glasses for High Power Lasers
Principal Investigator: Dr Kristina Lipinska, University of New Mexico, CHTM, Albuquerque, NM 87106, USA
Period of Performance: 2016-2019

I. Project Overview

High-power, rare-earths (REs) doped fiber lasers with a glass-based functional core are used in numerous commercial applications, such as telecommunications, as well as in those relevant to DoD missions. They require intense light for directed energy applications and for propagation over long distances within atmospheric transmission windows [1]. When considering REs-doped glasses for high-power laser applications, the phenomenon of photodarkening remains the key issue in limiting a fiber's optical performance. Photodarkening is an irradiation-induced gradual increase of a glass fiber's absorption, which reduces its light transmission capability and decreases the fiber's power output over time. It is a critical factor in limiting fiber laser operation, degrading device performance and shortening its lifetime. There are contradictory opinions about the mechanism of photodarkening and there is no clear explanation for its microscopic origin. Several explanations have been given so far that are either inspired by experimental observations or aimed at rationalizing experimental findings [2-10].

While the exact photodarkening mechanisms still remain open, it is recognized that this phenomenon may be correlated to the presence of different types of oxygen-deficiency centers (ODCs) and/or the formation of color centers (a trapped charge, i.e. an electron or a hole, which is trapped by defects within the glass matrix). However, no study has definitely identified those color centers or explained the route leading to photodarkening. One hypothesis could be that rare-earth (for example Er^{3+}) clustering causes photodarkening in a multi-step, multi-photon absorption process, where several excited cluster ions co-operate to supply energy for capturing electrons and holes at different structural defects. The complexity of the situation is reflected by the fact that despite numerous studies, we are still unable to pinpoint what is happening in a glass fiber exposed to high power laser [8, 10-15]. It is the lack of knowledge on the relationship between photodarkening on one side, and the microstructural and chemical modifications in the glass networks on the other side, that constitutes a missing link and prevents us from understanding of the detailed structural pathways for the complex optical response leading to photodarkening.

One should note that the most effective strategy for moving towards a solution to the issues of REs clustering and glass fibers photodarkening effect cannot be unidirectional, but requires related research issues to be addressed in concert: (1) the control of local order or microstructure of host glass network, (2) the control of level of rare-earths doping and (3) the control of local structural environment of functional atoms in a glass architecture.

In this project, and in relation to photodarkening, we address the missing links connecting: on one side glass chemistry and glass network microstructure, including local structural environment around selected atoms, and on the other side rare-earths clustering effects and optical transmission losses. This is achieved by leveraging a multi-technique experimental approach.

The novelty of our project is in approaching the problem from the materials science point of view. The strategy implemented by us includes synthesis of sets of custom designed, non-esoteric model glass materials, acquisition of information about their microstructure, optical properties and study of formation of microstructural and optically-active defects. Those defects generate alterations in the architecture of glass networks and modify the glass light transmission efficiency. Specifically, we explore in detail laser irradiation-driven structural changes in our model glass systems with and without rare-earths dopants. We focus on microstructural modifications of the glass networks resulting from variable rare-earths (Er^{3+}) concentration and from variable laser exposure conditions. The exposure of glasses to laser irradiation drives photoinduced bond-breaking and material densification, leading to an increase of the refractive index as well as to the formation of optically-active defect centers that are closely related to photodarkening phenomena.

The strategy of this project was: (i) to fabricate good optical quality model glasses, doped with heavy metal oxides, with different type of network formers, susceptible to accommodate variable levels of a luminescent dopant - Er^{3+}; (ii) to identify the microstructure of glass networks: main building blocks, connectivity; (iii) to evaluate the correlation between variable glass chemistry and glass network structure on the one hand and the formation of defect centers and the decrease in the materials' light transmission properties; (iv) to develop an understanding of the underlying photo-chemical mechanisms of the observed light transmission losses.

The overarching motivation for this project was to extend the current understanding of the complex relationships between microstructure and chemistry of a glass network, the connectivity of glass building blocks and its macroscopic optical performance. In the long term, our findings will improve the understanding of microstructural defects and of optically-active defects in glass networks and show a pathway to mitigate photodarkening. This knowledge will lay some solid stepping stones and will push the envelope in getting us closer towards a practical solution for the problem of rare-earths concentration-related and defect-related performance limits in glasses for optical fibers.

II. Fabrication of Materials

Glass compositions

The glass materials synthesized for this project belong to "model" glass systems, containing heavy metal oxides and varying types of glass network formers, in addition to different levels of rare-earth doping. The choice of heavy metal oxide glasses, as opposed to conventional silicate glasses, was motivated by their better solubility for rare-earth ions, lower phonon energy, good IR transmission and higher refractive index. The glass systems selected for this project also embody the essence of good glass network formers (silica and germania) and compatible dopants (potassium, gallium), have good thermal stability and mechanical stability, and present different microstructures. And yet they are simple enough for us to search for the basic mechanisms ruling optical properties.

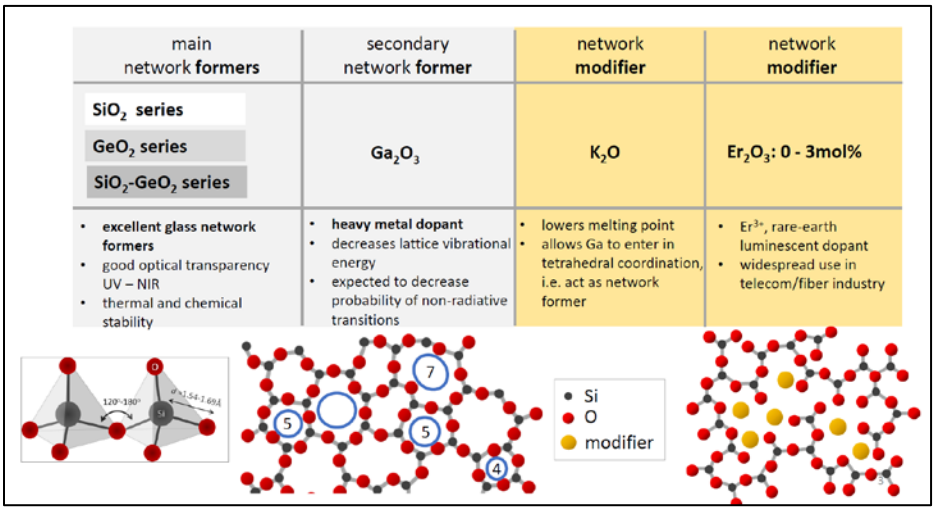

Table 1. Glass materials fabricated for this project: several isostructural glass systems; 14 glass compositions with and without luminescent rare-earth dopant.

The glasses were composed of isostructural, but chemically different, strong glass formers, and their microstructure was varied by adjusting the relative ratios of individual components (Table 1). The first system was comprised of silica-based glasses, the second system was comprised of germania-based glasses while the third system was comprised of mixed silica-germanate glasses. All glasses were doped with heavy-metal gallium and co-doped with a variable concentration of the luminescent dopant i.e. Er^{3+}. The strategy was to lower the phonon energy with respect to pure SiO_2 glass in order to enhance erbium radiative transitions, while maintaining a non-esoteric chemistry that is compatible with silica-based optoelectronic devices (Table 1 and [16-17]).

Glass synthesis

For glass synthesis, a mixture of initial batch components will be prepared using analytical grade reagents (99.999% purity) to avoid any spurious effects of unwanted luminescent or other contaminants, found in lower purity reagents. The batch components were thoroughly ground, mixed, sintered, re-ground and re-sintered at low temperature and afterwards melted in alumina crucible at high temperature in research grade, programmable furnace in an air atmosphere. The liquid melts were rapidly cooled to obtain glasses. The fabricated glasses were annealed at low temperature, below glass transition points, to remove internal

stresses. For optical measurements bulk glass samples were cut into platelets and optically polished (Figure 1).

Fig. 1. The synthesis route of glass materials: low-temperature sintering of batch components, high-temperature melting, rapid-quenching.

III. Experimental Techniques

Glass materials characterization

The target areas for characterization of the glass materials were: microstructure of glass network, connectivity of glass building blocks, light emission properties in function of luminescent dopant concentration, local structural environment around functional components i.e. atoms, their spatial distribution and optical properties.

What?	How?	Details
Before irradiation **microstructure and Er^{3+} emission properties**	micro-Raman spectroscopy & luminescence spectroscopy	basic structural units, network connectivity, ring structures emission: Er^{3+}
Before irradiation **local order in glass, coordination of Er^{3+} and Ga^{3+}**	XAFS - synchrotron x-ray absorption fine structure spectroscopy	identification of **Er** and **Ga**, first, second neighbors, coordination
After irradiation **changes in microstructure of glass network**	fs-laser irradiation & micro-Raman spectroscopy	ring structures, glass densification
After irradiation **changes in emission properties-controlled creation of defects**	fs-laser irradiation & luminescence spectroscopy	emission: Er^{3+} and laser-generated defects (NBOHC)
During irradiation ***In situ* transmission loss, kinetics of defects formation**	fs-laser irradiation & *in-situ* transmission loss during laser irradiation	transmission losses versus glass chemistry; density of defects, kinetics

Table 2. A fully integrated, multi-technique approach to understanding the modification of glass networks, the local structural environment of functional glass components and laser-glass interactions leading to the formation of optically-active defect centers.

The main characterization techniques (Table 2) used were confocal micro-Raman spectroscopy, luminescence spectroscopy, transmission spectroscopy, also combined with controlled, pulsed laser irradiation using different laser sources and variable irradiation conditions and finally synchrotron x-ray absorption fine structure (XAFS) spectroscopy. Experimental details are in our publications [16-20].

IV. Project Achievements

A. Observation of quench-free enhanced emission in cluster-free, Er-doped heavy metal oxide glasses of our exclusive design

We successfully **demonstrated** a series of new, non-esoteric glass media (see Table 1) - of practical interest, because of their compatibility with silica – that accept high erbium concentrations and display an enhanced erbium emission, while limiting Er-Er clustering.

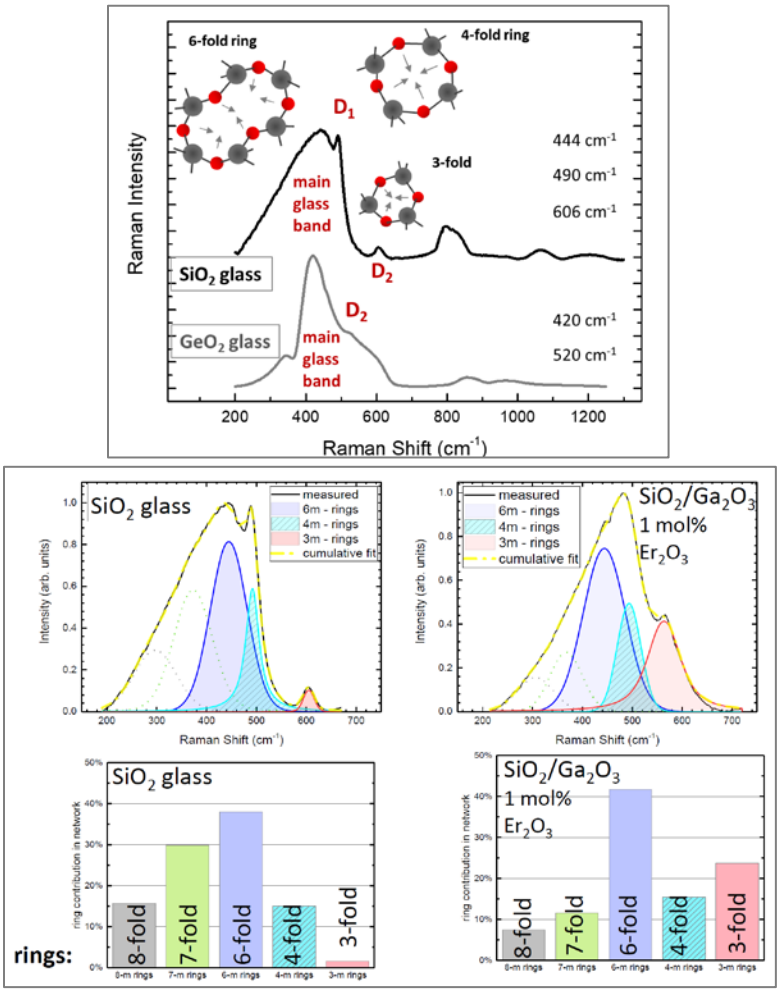

Fig. 2. *Top*: comparison of Raman spectra of reference SiO_2 and GeO_2 glasses. *Bottom*: Deconvolution of Raman bands showing the contribution of ring structures for a reference SiO_2 glass and for one of our glasses. Both for our glasses and for the reference SiO_2 glass, the 6-membered and larger tetrahedral rings dominate. However, our heavy-metal doped, erbium co-doped glass has a network built of fewer of the larger and more of the smaller than 6-fold rings.

We examined the effects of composition and microstructure of the glass networks on their optical properties. To understand the enhancement of emission in our glass materials we used Raman spectroscopy as a tool to develop a description of the glass' local microstructure. The deconvolution of Raman spectra illustrated how the spectral shape of the main Raman band can be used to extract information about the average ring structure (Figure 2). It is apparent that 6-membered and larger tetrahedral rings dominate for

both our glasses and a reference SiO_2 glass. However, our heavy-metal doped, erbium co-doped glass has a network built of fewer of the larger and more of the smaller than 6-fold rings. Both Raman spectroscopy and x-ray absorption fine structure spectroscopy [16] confirmed that gallium enters the glass network as a tetrahedral network former. In addition, the incorporation of gallium into the glass modified the energy landscape and created two distinct crystal field environments, which promoted Er^{3+} radiative transitions [16, 18].

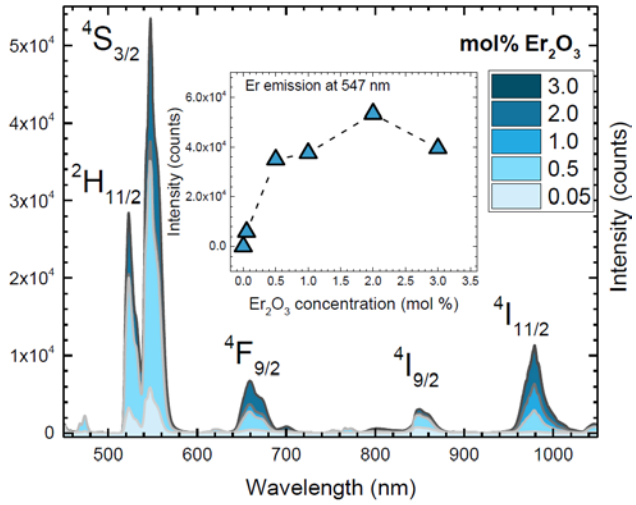

Fig. 3. Visible-infrared range of Er emission as a function of concentration. In the glass compositions of our design, we did not observe any quenching of emission up to 2 mol % of Er_2O_3, which corresponds to 4 mol % of Er^{3+}.

In the visible range (Figure 3 and [16]) an examination of the strong green emission band at ~550 nm ($^4S_{3/2} \rightarrow {}^4I_{15/2}$, Fig. 2(d)), reveals that in the '(Si)/Ga-series', emission initially slowly increases up to 2 mol% of Er_2O_3 and then drops at higher doping, indicating the onset of concentration quenching.

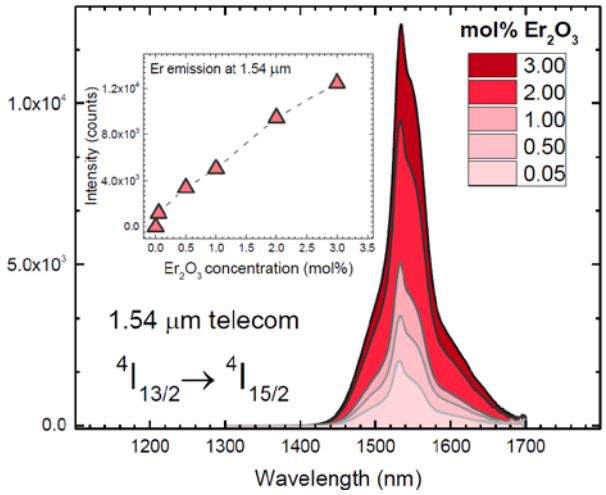

Fig. 4. Near-infrared, telecom Er emission at 1.5 um ($^4I_{13/2} \rightarrow {}^4I_{15/2}$) as a function of Er_2O_3 concentration. In the glass compositions of our design, we did not observe any quenching of the 1.54 µm emission up to 3 mol % of Er_2O_3, which corresponds to 6 mol % of Er^{3+}.

In the NIR range (Figure 4) the levels of Er_2O_3 doping without emission quenching are better than those reported for other oxide glasses, such as alumino-silicate, phosphate or chalcogenide glasses. At the ~1.5 μm telecom emission there is no sign of luminescence quenching up to 3 mol% of Er_2O_3 (Fig. 4 and [16]). This is a noteworthy outcome and since the close-to-linear trend of increasing intensity does not show signs of tapering off, it could imply that higher Er_2O_3 doping could be accepted.

Our results point the way to designing host glass matrices that limit interactions between neighboring rare-earth ions (Er-Er interactions) and thus minimize loss of excitation by energy migration and maximize light output. Detailed knowledge of the relationship between the glass network structure and chemistry, as well as full understanding of the microstructural and optical roles of all components provides a path forward to develop higher performance glass-based optical devices, such as lasers and amplifiers.

B. Ultrafast laser-generated structural modifications in networks of isostructural but chemically different and Er-doped glass materials

The interaction between glass materials and femtosecond (fs) laser pulses can result in a variety of effects, including changes in: (i) local composition, (ii) valence states of certain ions, (iii) optical properties, as well as (iv) nucleation of nanoparticles and crystallization [21-23]. Understanding and controlling the processes governing such structural alterations in glasses is important for the fabrication of photonic structures. The most common substrate investigated frequently is pure amorphous silica, with focus on writing of optical waveguides [24-28].

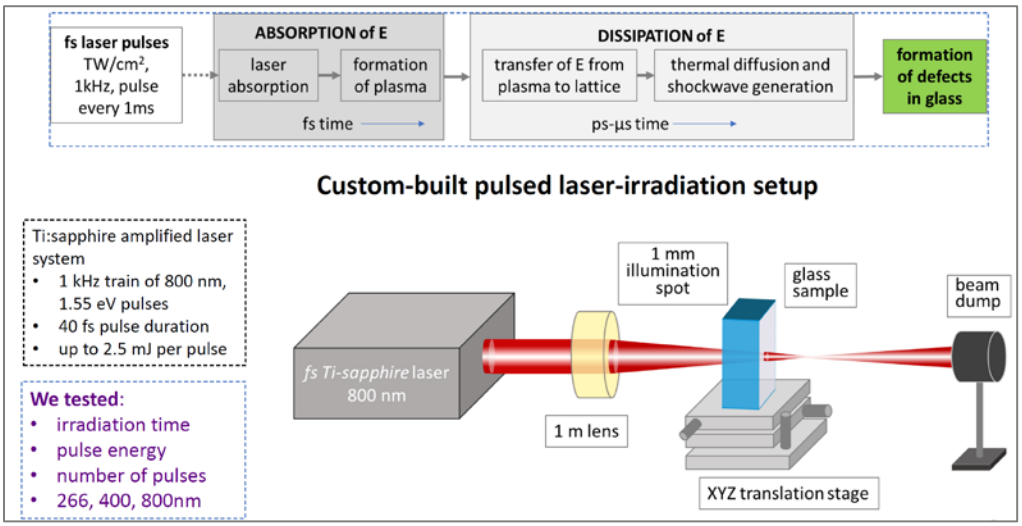

Fig. 5. Custom-built set-up for pulsed laser irradiation used for the controlled generation of defects in our glasses. Top inset shows the steps in the process of fs-laser irradiation leading to the formation of microstructural defects in the glass network.

A consistent picture of fs-laser induced alterations, the mechanisms linked to the creation of microstructural defects and of defect-assisted densification in different glass networks still remains elusive. When a glass medium is additionally doped with luminescent rare-earths ions (REs), fs-laser processing can be used to fabricate high-gain optical devices, such as waveguide lasers and waveguide amplifiers [29-32]. The majority of studies that report on monitoring of fs-laser created defects in glasses have focused only on un-doped glasses, mostly silicate or phosphate compositions [24-30]. In fact, when a glass is doped with Er^{3+},

the fundamental study of optically active defects becomes very challenging. This is because the strong emission bands of Er^{3+}, spanning from visible to infrared, dominate over the emission signatures (luminescence), which are used to monitor the formation of fs-laser created defects [17].

We investigated the effects of femtosecond, multi-pulse laser exposure on the structural changes in a series of our Er^{3+}-doped glasses. We analyzed microstructural alterations in the glass network and we monitored the formation of defect centers resulting from variable laser exposure conditions (Figure 5 and [17]).

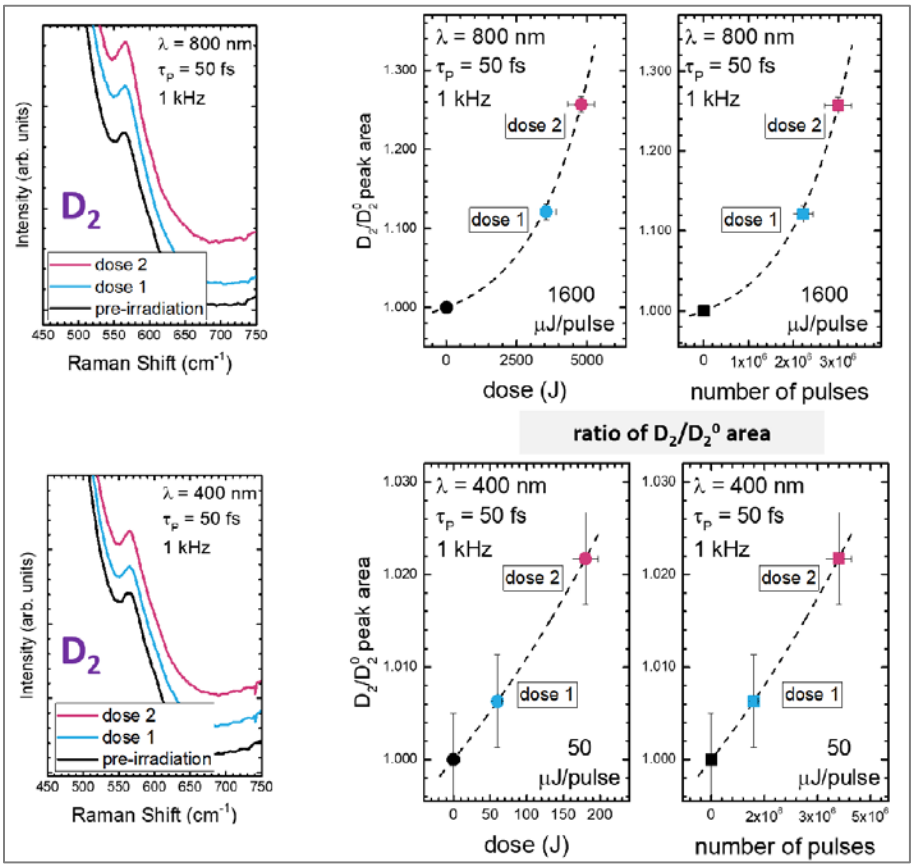

Fig. 6. Densification of glass microstructure probed by Raman. Comparison of Raman spectra of pre- and post-irradiated glasses. Different irradiation doses at 400 nm versus 800 nm, that control the laser energy delivered to the sample. For both 400 and 800 nm irradiation, glass densification depends on the photon dose used. D_2 bands mark the contribution of the smallest 3-fold tetrahedral rings.

First, we induced and subsequently probed, using Raman spectroscopy, the subtle differences in the glass network architecture, which are generated by different laser wavelengths and at different doses. (Figure 6). Next, using luminescence spectroscopy, we monitored the fs-laser driven formation of optically-active defects in the glass network. Finally, we demonstrated how to decouple the luminescence signals of laser-induced optically-active defects from the much stronger and usually dominating emission of Er^{3+} (Figure 7, Figure 8 and [17]).

The results of Raman studies can be summarized into a few key findings (Figure 6). Femtosecond laser exposure of Er^{3+}-doped and heavy-metal co-doped oxide glass, leads to various degrees of microstructural reorganization in the network. Specifically, in the short-to-medium range order, such exposure generates

an increasing number of small, i.e. 3- and 4-fold tetrahedral rings in the backbone of the irradiated volume of the glass. The formation of such low-dimensional, strained rings occurs at the expense of 6-fold and larger rings, increases connectivity of the network and leads to the creation of a more compacted network, meaning glass densification.

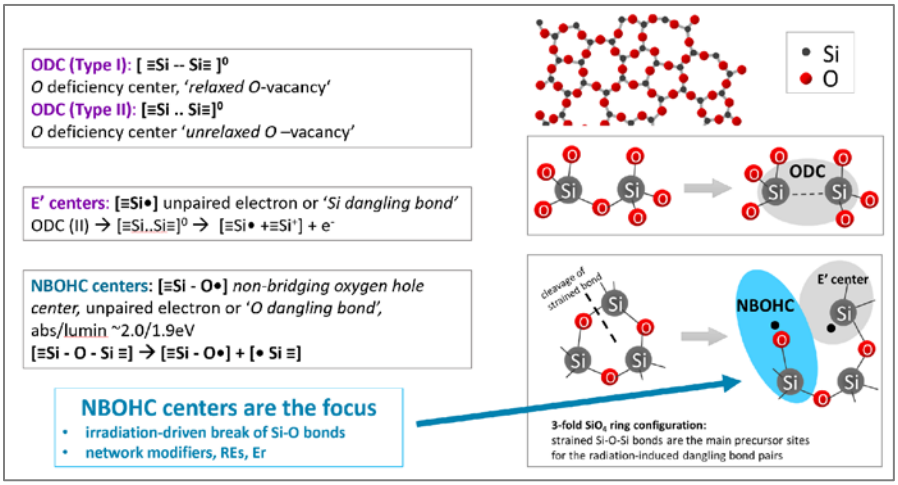

Fig. 7. Most common types of defects in glasses.

Irradiation can generate different types of defects in glass by breaking of bonds in the network. We focus here on the search for optically active defects that have a spectral signature in the visible range of emission and on type of defects called non-bridging oxygen hole centers (NBOHC, Figure 7)) they are important for the fabrication of optical devices written in glass [17].

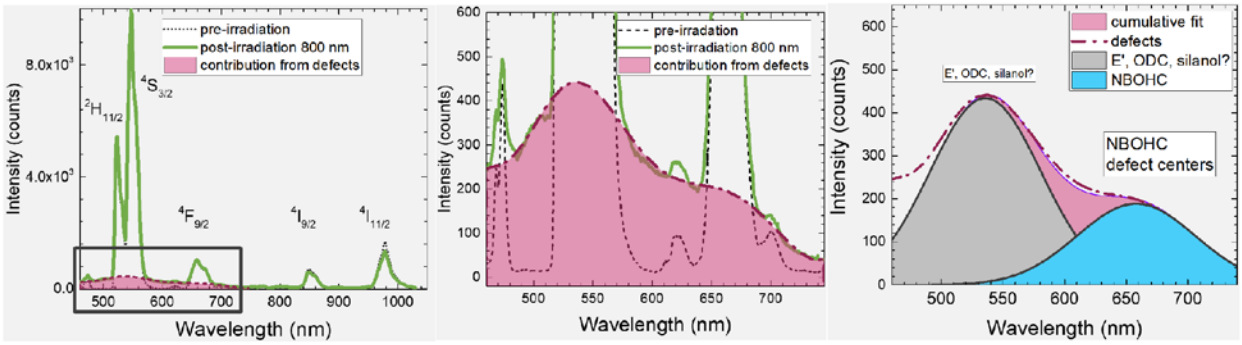

Fig. 8. Luminescence spectra of glasses before and after 800 nm fs-laser irradiation, at the highest dose (1kHz, 40 ns, 50 mJ/pulse) [17]. Left: full luminescence spectrum dominated by the typical Er emission. Center: zoom on the region of interest where we observe the emission form MBOHC defects. Right: a Gaussian deconvolution of the irradiation-generated background, showing the contribution from NBOHCs as well from unknown defects. The outcome of irradiation at 800nm is: (i) bond breaking in glass network and (ii) formation of Non-Bridging-Oxygen-Hole-Centers.

Luminescence spectroscopy allowed us to monitor the formation of optically active defects (Figure 7) in the irradiated volume of the Er^{3+}-doped glass (Figure 8)

We demonstrated how to decouple the very weak luminescence signals of laser-generated optically-active defects from the dominating emission of Er^{3+}. We elucidated the relationship between the initial and the irradiation-modified glass microstructure, including bond breaking, the formation of optically active defects and defect-assisted densification build-up in the glass network [17].

Femtosecond laser exposure ultimately brings a gradual, defect-driven glass network densification within the laser-irradiated volume. This study extends our understanding of fs-laser irradiation-driven structural modifications and demonstrates defect monitoring in Er^{3+}-doped oxide glasses.

To the best of our knowledge, no study has reported the detection of luminescence from defect centers in glasses, when an Er^{3+} dopant is also present. In fact, strong emission bands of typical Er^{3+} radiative transitions can overwhelm the weak intensity luminescence signals from irradiation-created defect centers, when those signals occur in the same spectral range [31, 33-34]. In this work we are able to successfully decouple the very weak luminescence of laser-generated defects from the dominating luminescence of Er^{3+}.

C. Kinetics of defect formation: transmission losses during fs-irradiation

We studied the irradiation-driven losses in transmission signal in various glasses during fs-laser irradiation. The goal was to quantify the kinetics of formation of defects, specifically: the defect saturation time, the relative rate of defects formation and the density of defects for different glass matrices.

We built a custom optical set-up for measuring *in situ* and in real time, the kinetics of formation of defects during fs-laser irradiation. To generate defects in glass we used a fs laser at 800 nm delivering a 1 kHz train of pulses of 2.5 mJ energy/pulse. To monitor transmission losses through a glass as a function of irradiation time we used a 100 kHz, 430 nm photodiode [19].

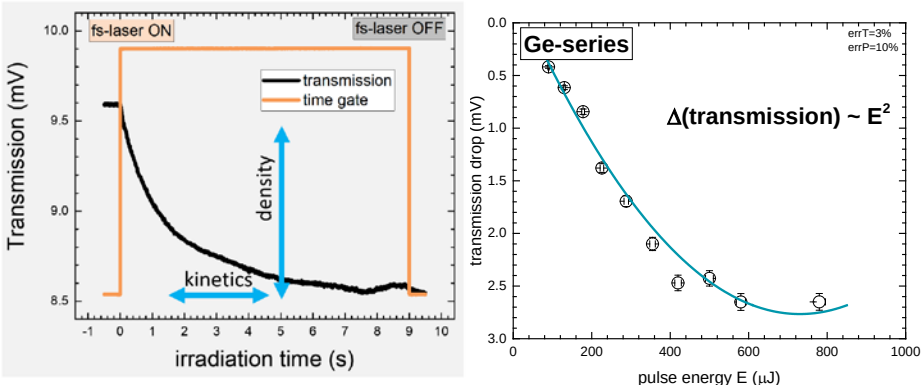

Fig. 9. *Left:* A typical signal of transmission loss versus fs laser exposure time. Arrows indicate how quantification of time (kinetics) and of density of defects generated by the irradiation process can be extracted. *Right*: Transmission loss as a function of energy for one of our glasses.[19]

We performed single point transmission measurements during 800 nm, fs-laser irradiation, for different irradiation doses, different pulse energies and different glasses. Figure 9 shows a typical signal of transmission loss versus fs laser exposure time. Transmission loss is a measure of the number of defects created by fs laser-irradiation. We found that for all glasses the transmission signal loss occurs at a very fast time scale (a few seconds). The kinetics of creation of defects is characterized by 3 stages: fast decrease of transmission, followed by slower decrease and finally a plateau [19].

The magnitude of transmission drop is a function of laser pulse energy for all glasses. For our Si-based and Ge-based glass systems we found that the transmission loss scales only as E^2, as shown in Figure 9. We identified in literature one comparable study of commercial boro-silicate glass. In that study it was found that in the boro-silicate glass the transmission drop scales as $E^{14.6}$, hence is extremely sensitive to laser pulse energy. **We demonstrated** that, remarkably, our glasses are much less sensitive to pulse energy, meaning they can handle much higher laser powers, which is an advantage for practical applications [19].

D. Microscopic model of Er^{3+} environment in heavy-metal silica glasses by XAFS spectroscopy: network former mixing effects

We investigated a series of erbium-doped and gallium-co-doped silica-based glasses using synchrotron x-ray absorption near-edge structure (XANES) and extended x-ray absorption fine structure (EXAFS) spectroscopies [18, 20]. We used these two techniques to explore the effect of dopants on the medium range order of the glass network. Specifically, the objective was to understand the effect of gallium on the local environment of erbium in the glass network which, in turn, will affect the emission properties of Er^{3+}. Experiments were carried out at the facilities of the MRCAT beamline [35-36] at the Advanced Photon Source of Argonne National Laboratory (Chicago, IL).

Regardless of the presence or absence of long-range order in a material, the spectral shape in the element-selective XANES, provides a picture of the electronic properties (i.e. oxidation state) and of the local geometry (i.e. coordination chemistry) of the element studied.

The element-selective EXAFS spectroscopy is highly sensitive to the short-range order in a material. A detailed analysis of EXAFS data, based on the multiple scattering formalism, allows to describe the local structural order around the selected atom i.e. erbium and gallium atoms in our glasses.

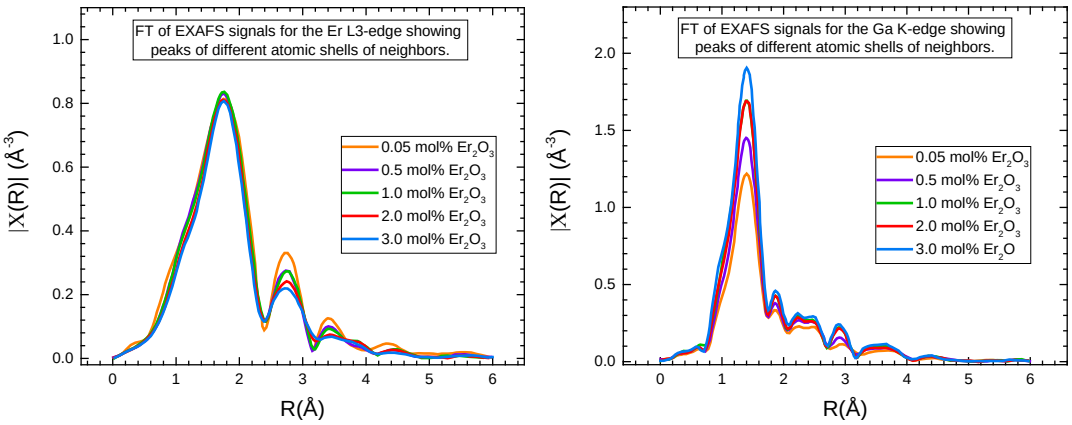

Fig. 10. Left: Er edge XAFS results. Right: Ga edge XAFS results. Details are in [18, 20].

Figure 10 shows a summary of XAFS results, for one of our glasses. Figure 11 shows a sketch representative of the local environment of Er^{3+} and Ga^{3+} that is based on a quantitative analysis of the scattering paths and occupancies of EXAFS data. At all erbium concentrations EXAFS data show only Er-O, Ga-O and Ga-O-[Er/Ga] interactions, with no detectable contribution of direct Er-Er or Er-Si or Ga-Si correlations up to ~4 Å, that is up to two nearest neighbor coordination shells [18, 20].

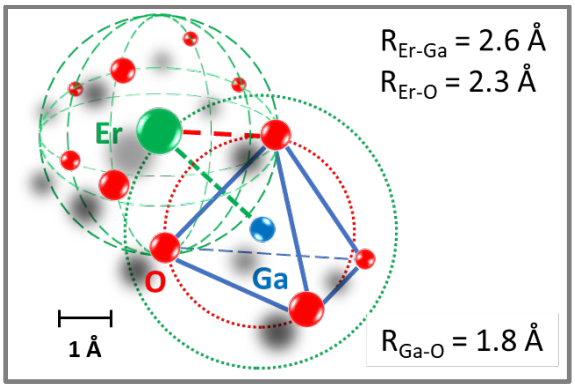

Fig. 11. Model of the short-range order in our erbium-doped and gallium-co-doped silica-based glass. The local environment of Er and Ga is based on quantitative analysis of XAFS results.

In our glasses the solubility of erbium is markedly increased and in EXAFS we detect the formation of Ga-O-[Er/Ga] rich regions, which are similar to the Er-Al complexes proposed by Lægsgaard [37], or the solvation-shell model by Arai [38]. It appears that Ga^{3+} plays a role similar to Al^{3+} in our glasses: in order to enter a tetrahedral coordination with oxygens (GaO_4), Ga is being charge-compensated by Er^{3+}. In fact, EXAFS confirms that Ga and Er are located in proximity. In the second shell of Ga, the fractional occupancy of Er is ~0.4. In other words, there is 1 Er per ~ 2.5 GaO_4 tetrahedra. We suggest that in our glasses 1 Er^{3+} can charge-compensate 2.5 Ga^{3+}. This process of charge compensation allows the Er ions to fit better within an otherwise 'inhospitable' silica glass network. In Figure 4 (presented in section A) there is no decrease of luminescence intensity with increasing Er^{3+} concentration, i.e. no quenching up to 6 mol% of Er^{3+}. This favorable outcome is well explained by our EXAFS results: the proximity of Er to where Ga is found, as well as the formation of Ga-O-[Er/Ga] rich domains within the SiO_4 tetrahedral network, create a more energetically favorable environment for Er^{3+} ions [18, 20].

We demonstrated, using EXAFS, that Er^{3+} prefers Ga^{3+}- rich domains. Our XANES findings and presence of isosbestic points show that the incorporation of Ga into the glass matrix results in a modification of the energy environment of Er atoms i.e. gallium likely increases the diversity of erbium energy sites. Put together these results point to the idea that gallium's role within the glass network is to counteract the clustering of Er^{3+}, and to prevent luminescence concentration quenching by decreasing the probability of detrimental non-radiative Er - Er energy transfer processes.

V. What Are Our Accomplishments?

- Designed and synthesized several isostructural, non-esoteric glasses, variably doped with Er^{3+}
- Quantified the glass network microstructures, local environments (synchrotron EXAFS spectroscopy) around target atoms
- Achieved quench-free emission, from Er^{3+}-doped, cluster-free glasses of our invention in NIR and in visible spectral ranges
- Assessed how pulsed-laser irradiation affects the glass network and creates optically-active defect centers and generates glass (network) densification
- Appraised how variable wavelengths, pulsed-laser irradiation affects the glass network and creates defects i.e. defect centers related closely to photodarkening effect observed in glass cores of optical fibers
- Quantified how pulsed-laser irradiation affects the glass light transmission properties and quantified the density of those defects and more importantly the kinetics of defect formation, all in custom-made glass materials

VI. Published papers and papers in preparation

K. Lipinska, F. Cavallo, J-L Ayitou, C. Segre: Quench-free enhanced emission in cluster free Er-doped heavy metal oxide glasses, Optical Mat. Express 9 (3) 2019

K. Lipinska, L. Emmert, F. Cavallo, J-C. Diels: Ultrafast laser-generated structural modifications in an Er-doped heavy metal oxide glass, Optical Mat. Express 9 (5) 2019

K. Lipinska, C. Segre: Microscopic model of Er^{3+} environment in heavy-metal silica glasses: network former mixing effects, to be submitted to J. Appl. Phys.

K. Lipinska, L. Emmert: Kinetics of defect formation in fs-laser irradiation in heavy-metal glasses, in preparation

VII. Presentations

K. Lipinska, “Fundamental Studies of Heavy Metal Oxide Glasses for High Power Lasers”, 2017 Program Review of Aerospace Materials for Extreme Environments, May 15-19, 2017, KAFB, NM

K. Lipinska, “Fundamental studies of Er-doped heavy metal oxide glasses: glass networks, generation of defects and optical properties related to photodarkening.”, 2018 Program Review of Aerospace Materials for Extreme Environments, May 14-18, 2018, Niceville, FL.

K. Lipinska, “Study of Er-doped glasses: microstructure, optical properties and laser-generated defects related to photodarkening”, 2019 Joint AFOSR & NSF Program Review: Quantitative Representation of Microstructure and Materials for Extreme Environments. May 20-24, 2019, Alexandria, VA

Project collaborators

Dr. Jean-Claude Diels, University of New Mexico
Dr. Luke Emmert, University of New Mexico
Dr. Carlo Segre, ANL-Advanced Photon Source (MRCAT beamline) and Illinois Institute of Technology (IIT)
Dr. Jean-Luc Aitou, Illinois Institute of Technology (IIT)
Dr. Francesca Cavallo, University of New Mexico

References

1. Jackson, S.D., Towards high-power mid-infrared emission from a fibre laser. Nature Photonics, 2012. 6(7): p. 423-431.
2. Miniscalco, W.J., Erbium-Doped Glasses for Fiber Amplifiers at 1500-Nm. Journal of Lightwave Technology, 1991. 9(2): p. 234-250.
3. Jetschke, S., et al., Efficient Yb laser fibers with low photodarkening by optimization of the core composition. Optics Express, 2008. 16(20): p. 15540-15545.
4. Muller, H.R., et al., Fibers for high-power lasers and amplifiers. Comptes Rendus Physique, 2006. 7(2): p. 154-162.
5. Skuja, L., Optically active oxygen-deficiency-related centers in amorphous silicon dioxide. Journal of Non-Crystalline Solids, 1998. 239(1-3): p. 16-48.
6. Stevens-Kalceff, M.A. and J. Wong, Distribution of defects induced in fused silica by ultraviolet laser pulses before and after treatment with a CO(2) laser. J. Applied Physics, 2005. 97(11).
7. Glebov, L.B., Linear and nonlinear photoionization of silicate glasses. Glass Science and Technology, 2002. 75: p. 1-6.
8. Engholm, M., L. Norin, and D. Aberg, Strong UV absorption and visible luminescence in ytterbium-doped aluminosilicate glass under UV excitation. Optics Letters, 2007. 32(22): p. 3352.
9. Simon, S. and V. Simon, Thermal characterization of gallium-bismuthate oxide glasses. Materials Letters, 2004. 58(29): p. 3778-3781.
10. Crivelli, B., et al., Photoinduced conversion of optically active defects in germanium-doped silica. Physical Review B, 1996. 54(23): p. 16637-16640.
11. A.D. Guzman Chavez, et al., Reversible photo-darkening and resonant photobleaching of Ytterbium-doped silica fiber at in-core 977-nm and 543-nm irradiation. Laser Phys. Lett., 2007. 4: p. 734.
12. Engholm, M. and L. Norin, Preventing photodarkening in ytterbium-doped high power fiber lasers; correlation to the UV-transparency of the core glass. Optics Express, 2008. 16(2): p. 1260.
13. Taccheo, S., et al., Concentration dependence and self-similarity of photodarkening losses induced in Yb-doped fibers by comparable excitation. Optics Express, 2011. 19(20): p. 19340.
14. Dianov, E.M., D.S. Starodubov, and A.A. Frolov, UV argon laser induced luminescence changes in germanosilicate fibre preforms. Electronics Letters, 1996. 32(3): p. 246-247.
15. Arai, K., et al., Evidence for Pair Generation of an E' Center and a Nonbridging Oxygen-Hole Center in Gamma-Ray-Irradiated Fluorine-Doped Low-Oh Synthetic Silica Glasses. Physical Review B, 1992. 45(18): p. 10818-10821.
16. K. Lipinska, F. Cavallo, J-L Ayitou, C. Segre: Quench-free enhanced emission in cluster free Er-doped heavy metal oxide glasses, Optical Mat. Express 9 (3) (2019)
17. K. Lipinska, L. Emmert, F. Cavallo, J-C. Diels: Ultrafast laser-generated structural modifications in an Er-doped heavy metal oxide glass, Optical Mat. Express 9 (5) (2019)
18. K. Lipinska, C. Segre: Microscopic model of Er^{3+} environment in heavy-metal silica glasses: network former mixing effects, to be submitted to J. Appl. Phys.
19. K. Lipinska, L. Emmert: Kinetics of defect formation in fs-laser irradiation in heavy-metal glasses, in preparation
20. K. Lipinska, “Study of Er-doped glasses: microstructure, optical properties and laser-generated defects related to photodarkening”, 2019 Joint AFOSR & NSF Program Review: Quantitative Representation of Microstructure and Materials for Extreme Environments. May 20-24, 2019, Alexandria, VA
21. R. R. Gattass and E. Mazur, “Femtosecond laser micromachining in transparent materials,” Nature Photon. 2, 219-225 (2008).

22. K. Miura, J. Qiu, T. Mitsuya, K. Hirao, “Space-selective growth of frequency-conversion crystals in glasses with ultrashort infrared laser pulses,“ Opt. Lett. 25(6), 408-410 (1999).
23. J. R. Qiu, M. Shirai, T. Nakaya, J. Si, K. Hirao, “Space-selective precipitation of metal nanoparticles inside glasses, “Appl. Phys. Lett. 81, 3040-3042 (2002).
24. W. Chan, T. R. Huser, S.H. Risbud and D. M. Krol, “Modification of the fused silica glass network associated with waveguide fabrication using femtosecond laser pulses,” Appl. Phys. A 76, 367-372 (2003).
25. J. Hernandez-Rueda, J. Clarijs, D. van Oosten, and D. M. Krol, “The influence of femtosecond laser wavelength on waveguide fabrication inside fused silica,” Appl. Phys. Lett. 110, 1611091-1611095 (2017).
26. J. J. Witcher, W. Reichman, L. B. Fletcher, N. W. Troy and D. M. Krol, "Thermal annealing of femtosecond laser written structures in silica glass'" Opt. Mat. Exp. 3(4), 502-510 (2013).
27. A. M. Streltsov and N. F. Borrelli, “Study of femtosecond-laser-written waveguides in glasses,” J. Opt. Soc. Am. B 19(10), 2496-2504 (2002).
28. L. B. Fletcher, J.J. Witcher, N. Troy, S.T. Reis, R.K. Brow, R. M. Vazquez, R. Osellame, and D. M. Krol, “Femtosecond laser writing of waveguides in zinc phosphate glasses,” Opt. Mater. Express 1(5), 845-855 (2011)
29. G. Della Valle, R. Osellame, and P. Laporta, “Micromachining of photonic devices by femtosecond laser pulses,” J. Opt. A: Pure Appl. Opt. 11, 013001-013019 (2009).
30. R. Osellame, G. Della Valle, N. Chiodo, S. Taccheo, P. Laporta, O. Suelto, and G. Cerillo, “Lasing in femtosecond laser written optical waveguides,” Appl. Phys. A 93, 17–26 (2008).
31. L. B. Fletcher, J.J. Witcher, N. Troy, S.T. Reis, R.K. Brow, and D. M. Krol, “Effects of rare-earth doping on femtosecond laser waveguide writing in zinc polyphosphate glass,” J. Appl. Phys. 112, 0231091-0231096 (2012).
32. N. D. Psaila, R. R. Thomson, H. T. Bookey, A. K. Kar, N. Chiodo, R. Osellame, G. Cerullo, A. Jha, and S. Shen, “Er:Yb doped oxyfluoride silicate glass waveguide amplifier fabricated using femtosecond laser inscription,” Appl. Phys. Lett. 90, 131102-131106 (2007).
33. L. B. Fletcher, J. J. Witcher, N. Troy, R. K. Brow, and D. M. Krol, “Single-pass waveguide amplifiers in Er-Yb doped zinc polyphosphate glass fabricated with femtosecond laser pulses,” Opt. Lett. 37(7), 1148-1150 (2012).
34. T. Toney Fernandez, G. Della Valle, R. Osellame, G. Jose, N. Chiodo, A. Jha, and P. Laporta, “Active waveguides written by femtosecond laser irradiation in an erbium-doped phospho-tellurite glass,” Opt. Express 16(19), 15198-15205 (2008).
35. A. J. Kropf, J. Katsoudas, S. Chattopadhyay, T. Shibata, E. A. Lang, V. N. Zyryanov, B. Ravel, K. McIvor, K. M. Kemner, K. G. Scheckel, S. R. Bare, J. Terry, S. D. Kelly, B. A. Bunker, and C. U. Segre, “The new MRCAT (Sector 10) Bending Magnet Beamline at the Advanced Photon Source,” AIP Conf. Proc. 1234, 299-302 (2010).
36. C. U. Segre N. E. Leyarovska, L. D. Chapman, W. M. Lavender, P. W. Plag, A. S. King, A. J. Kropf, B. A. Bunker, K. M. Kemner, P. Dutta, R. S. Duran and J. Kaduk, "The MRCAT Insertion Device Beamline at the Advanced Photon Source", CP521, Synch. Rad. Instr.: 11th U.S. National Conference, ed. P. Pianetta, 419-422, AIP, New York (2000).
37. J. Lægsgaard,” Dissolution of rare-earth clusters in SiO2 by Al codoping: A microscopic model,” Phys. Rev. B 65, 1741141-17411410 (2002).
38. K. Arai, H. Namikawa, K. Kumata, and T. Honda, "Aluminum or phosphorus co-doping effects on the fluorescence and structural properties of neodymium-doped silica glass," J. Appl. Phys. 59, 3430-3436 (1986).